# Near-Field Optical Studies of Thin-Film Mesostructured Organic Materials

DAVID A. VANDEN BOUT, JOSEF KERIMO, DANIEL A. HIGGINS,† AND PAUL F. BARBARA*

*Department of Chemistry, University of Minnesota, Minneapolis, Minnesota 55455*

Received October 21, 1996

Techniques in optical microscopy for thin-film analysis are undergoing a revolution to meet the challenges of analyzing complex thin films. These films range from biological examples, including cell membranes, to modern synthetic materials such as emitting layers in organic light-emitting diodes (LED), and highly organized, multilayer assemblies. All of these materials posses simultaneous and distinct organization on multiple distance scales, i.e., atomic, molecular, nanoscopic, mesoscopic, and in some cases even macroscopic. Among the most powerful emerging techniques for thin-film analyses is near-field scanning optical microscopy (NSOM). NSOM is a scanning probe optical microscopy that breaks the diffraction limit ($\lambda/2$) to the resolution of ordinary microscopy. This is achieved by illuminating (or collecting light from the sample) through a subwavelength aperture in a NSOM probe. The dramatic developments of NSOM in the 1980s and early 1990s have been reviewed.[1−5]

The most common NSOM probe is a tapered, aluminum-coated, single-mode optical fiber which has an aperture of a few tens of nanometers at one end. These probes offer optical resolution as small as 12 nm.[2] In NSOM the sample's lateral position in the *XY* plane is raster scanned while the sample/probe separation remains fixed (Figure 1). The NSOM tip/sample distance regulation mechanism provides a simultaneous scanning force microscopy (SFM) topographic image (similar to an AFM image) with the NSOM image. This leads to an informative correlation of the samples optical properties with its topography. The two most common types of NSOM images are transmission NSOM and fluorescence NSOM, which differ depending on whether all the light emanating from the tip/sample region, or only the excited fluorescence light, is collected. Spectroscopy with the NSOM probe is straightforward, allowing for both chemical contrast in the NSOM images and the study of the photophysics/photochemistry of the sample in localized regions. In particular, fluorescence NSOM is extraordinarily sensitive, leading to submonolayer observations and even single-molecule detection and spectroscopy.[6−11]

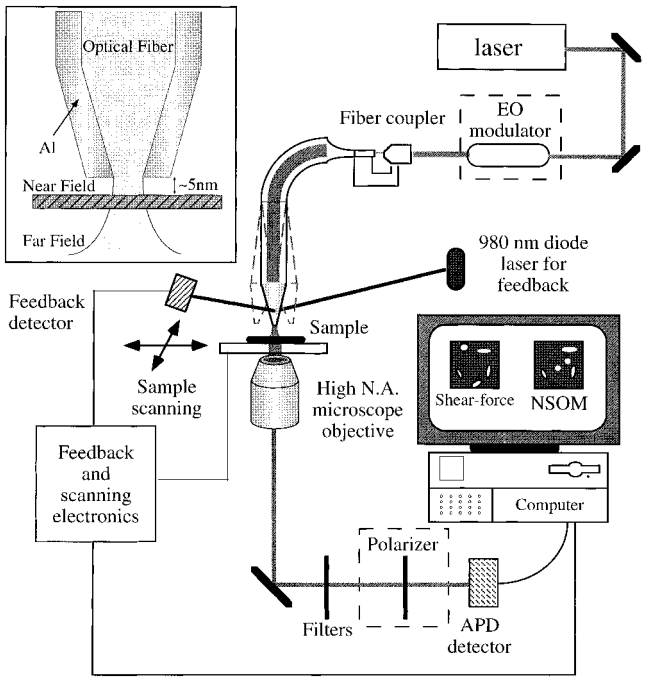


**FIGURE 1. Schematic of the NSOM apparatus.**

This Account reviews recent NSOM studies of functional organic thin-film materials that fluoresce. The paper focuses on how the mesostructure of a material modulates its spectroscopy and photophysics. We emphasize results from our laboratory. Many of the key advantages and fundamental principles of the NSOM

David A. Vanden Bout was born in New York, NY, in 1968. He received a B.S. in chemistry from Duke University in 1990 and a Ph.D. in Chemical Physics with Professor Mark Berg at the University of Texas at Austin in 1995. He is currently at the University of Minnesota as a NSF postdoctoral fellow under the direction of Professor Paul F. Barbara.

Josef Kerimo was born in Eregli, Turkey, in 1970. In 1993, he received his B.S. in chemistry from Baylor University. He is currently a graduate student at the University of Minnesota.

Daniel A. Higgins was born in Columbia, MO, in 1966. He received his undergraduate degree in chemistry from St. Olaf College (Minnesota) in 1988 and a Ph.D. in chemistry in 1993 with Professor Robert M. Corn at the University of Wisconsin—Madison. He recently completed a NSF postdoctoral fellowship with Paul F. Barbara at the University of Minnesota (1993−1996) and is currently at Kansas State University as an Assistant Professor of Analytical Chemistry.

Paul F. Barbara is a Professor of Chemistry at the University of Minnesota. He was born in New York, NY, in 1953 and attended Hofstra University, earning a B.A. in 1974. He received his Ph.D. in chemistry in 1978 from Brown University, working with R. G. Lawler, and carried out his postdoctoral work at Bell Laboratories with P.M. Rentzepis. In 1980, he joined the faculty of the University of Minnesota, achieving the rank of full professor in 1990. He was named 3M-Alumni Distinguished Professor of Chemistry in 1995. He is currently an Associate Editor of *Accounts of Chemical Research*, and Past Chair of the Division of Physical Chemistry of the American Chemical Society. His research interests include near-field scanning optical microscopy, the photophysics of DNA proton and electron transfer, and ultrafast chemical reaction dynamics in solution.

* To whom correspondence should be addressed.
† Kansas State University.

(1) Pohl, D. W. In *Advances in Optical and Electron Microscopy*; Mulvey, T., Sheppard, C. J. R., Eds.; Academic Press: New York, 1991; Vol. 12, p 243.
(2) Betzig, E.; Trautman, J. K. *Science* **1992**, *257*, 189.
(3) Kopelman, R.; Tan, W. H. *Appl. Spectrosc. Rev.* **1994**, *29*, 39.
(4) Heinzelmann, H.; Huser, T.; Lacoste, T.; Güntherodt, H.-J.; Pohl, D. W.; Hecht, B.; Novotny, L.; Martin, O. J. F.; Hafner, C. V.; Baggenstos, H.; Wild, U. P.; Renn, A. *Opt. Eng.* **1995**, *34*, 2441.
(5) Buratto, S. K. *Curr. Opin. Solid State Mater. Sci.* **1996**, *1*, 485.
(6) Betzig, E.; Chichester, R. J. *Science* **1993**, *262*, 1422.
(7) Moerner, W. E.; Plakhotnik, T.; Irngartinger, T.; Wild, U. P. *Phys. Rev. Lett.* **1994**, *73*, 2764.
(8) Trautman, J. K.; Macklin, J. J.; Brus, L. E.; Betzig, E. *Nature* **1994**, *369*, 40.
(9) Ambrose, W. P.; Goodwin, P. M.; Martin, J. C.; Keller, R. A. *Phys. Rev. Lett.* **1994**, *72*, 160.
(10) Xie, X. S.; Dunn, R. C. *Science* **1994**, *265*, 361.
(11) Xie, X. S. *Acc. Chem. Res* **1996**, *29*, 598.



S0001-4842(96)00274-9 CCC: $14.00 

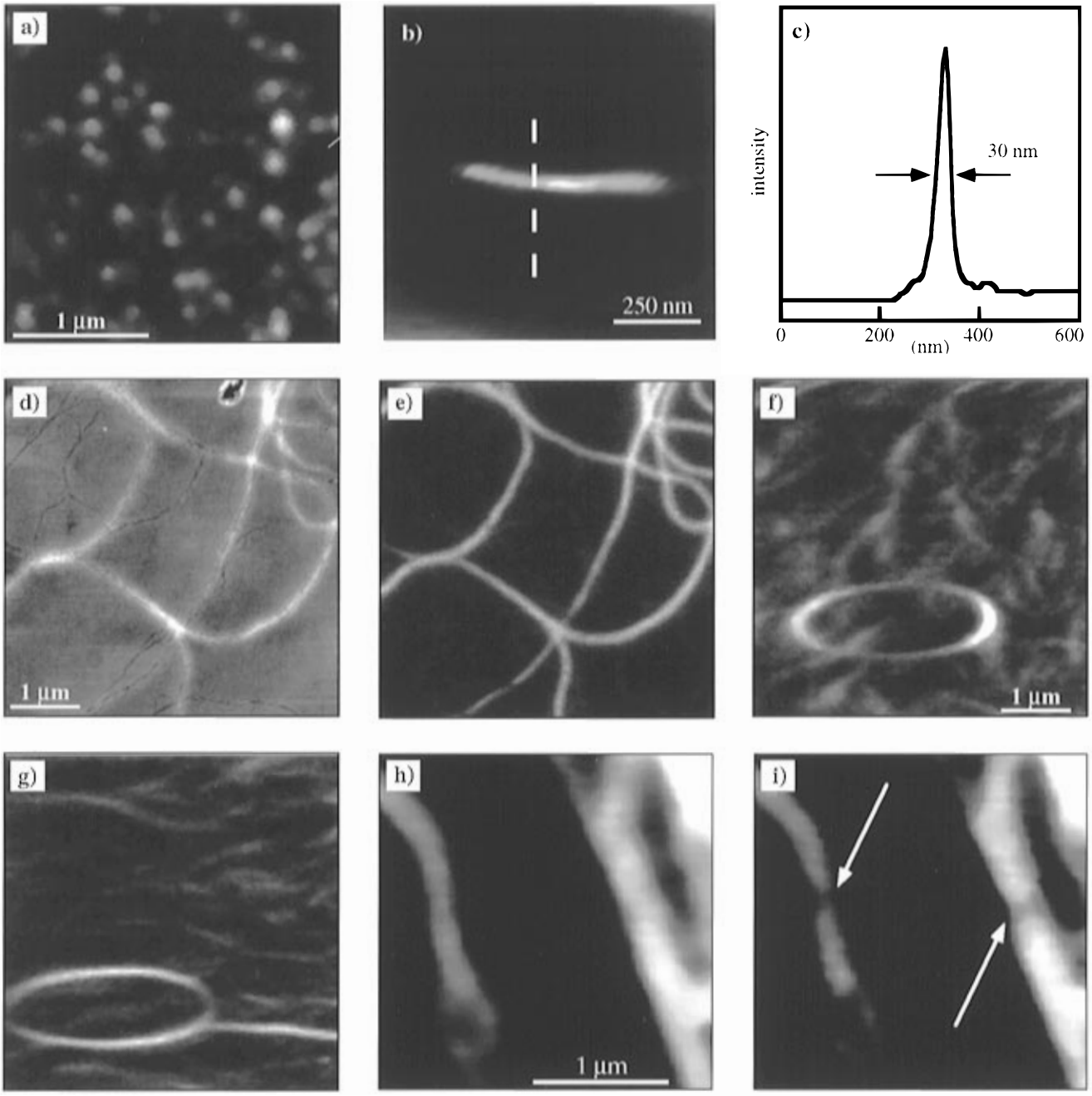


**FIGURE 2. (a) NSOM image of DiI single molecules. (b) NSOM image of a PPEI nanocrystal. (c) Line scan of a PPEI crystal. (d−i) Images of a PIC/PVS molecular yarn: (d) topography, (e) fluorescence NSOM, (f) vertical and (g) horizontal polarized fluorescence NSOM of the ring aggregate, (h) before and (i) after fluorescence NSOM images showing spatial hole-burning in a PIC/PVS aggregate fiber.**

technique for thin-film analysis had already been established in 1993, at the inception of our work. However, there were few real applications of the technique, especially for organics. In the work we review here, NSOM is found to work well in practice and to offer important new information on mesostructured organics, complementing the nonoptical methods of thin-film analysis such as SEM, TEM, STM, and AFM.

## NSOM Studies of Organic Thin Films

The interpretation of image contrast in NSOM is not straightforward due to the complex nature of the interaction of the sample with the near-field excitation. Nevertheless, for the types of samples described in this section, the NSOM images (with some key exceptions) are roughly higher spatial resolution versions of their far-field microscopy counterparts. For example, the fluorescence NSOM image is an estimate of the spatially resolved probe-induced fluorescence intensity, which itself is proportional to the product of the local absorbance and fluorescence quantum yield.

Our NSOM studies have employed a recently introduced NSOM instrument from Topometrix (Figure 1), which we have modified to allow for optical polarization analysis and single-molecule optical sensitivity. Both high sensitivity and polarization information are necessary for effective analysis of many materials. Figure 2a demonstrates the extreme sensitivity and spatial resolution of the apparatus for a "benchmark" sample of 1,1′-didodecyl-3,3,3′,3′-tetramethylindocarbocyanine (DiI) single mol-

ecules on a PMMA film.[6] The fluorescent regions are essentially images of the electric field distribution of the near-field tip, since the molecules are too small for the instrument to resolve. Therefore, the NSOM image of a molecule is a measure of the field size for the probe and the relative orientation of the molecule's transition moment and the direction of the probe's electric field. Tip aperture sizes and field distribution are typically 30−125 nm for fluorescence measurements depending on the required near-field intensity. The high excitation intensity required for single-molecule detection demands larger apertures. Therefore, the single molecules in Figure 2a show a resolution of approximately 125 nm. However, strongly emitting samples, like the single nanocrystal of the molecular semiconductor perylene bis(phenethylimide) (PPEI) shown in Figure 2b, can be imaged with smaller apertures. The line scan in Figure 2c shows the resolution in the crystal image is approximately 30 nm which corresponds to better than $\lambda/16$.

**A Molecular Yarn: Self-Assembled Fluorescent Fibers.** Aggregates of aromatic dyes have been at the center of the investigation of optical delocalization and electronic energy migration in organic materials.[12] The narrow intense visible absorption of many aggregates makes these systems useful in photographic sensitization, photocells, and natural and artificial photosynthesis. We became interested in the reports that polyionaphores, such as poly(vinyl sulfate) (PVS), greatly enhanced aggregate growth in aqueous solutions of the dye 1,1′-diethyl-2,2′-cyanine iodide (PIC). We saw this as a means to self-assemble networks of molecular aggregates in solution that could then be spin-coated on glass substrates to form permanent films. We were surprised to observe by NSOM that the resultant films were extensively ordered in long fluorescent, yarnlike aggregates that are a composite of the dye and PVS.[13−16] A schematic of this novel self-assembly structure is given in Figure 3a. Parts d−i of Figure 2 show NSOM images (both shear force and fluorescence) of various spin-coated samples of the molecular aggregates and PVS. Some of the fibers are resting on the surface of a PVS film while others are imbedded. Large-scale topography images show that the fibers are often hundreds of micrometers long and typically ∼50 nm thick. The fibers are themselves yarnlike composites of single dye threads.[15] The appearance of highly curved fibers indicates that the fibers are apparently quite flexible when they form in the liquid state.

Fluorescence NSOM images (Figure 2e) of the samples closely correspond to the topographic images (Figure 2d) of the exposed fibers, demonstrating that the dye is restricted to an aggregated state. Polarized-light-dependent imaging with NSOM provides further information on the molecular organization of the aggregates. Parts f and g of Figure 2 show the polarized emission in the horizontal and vertical directions for a continuous loop aggregate.

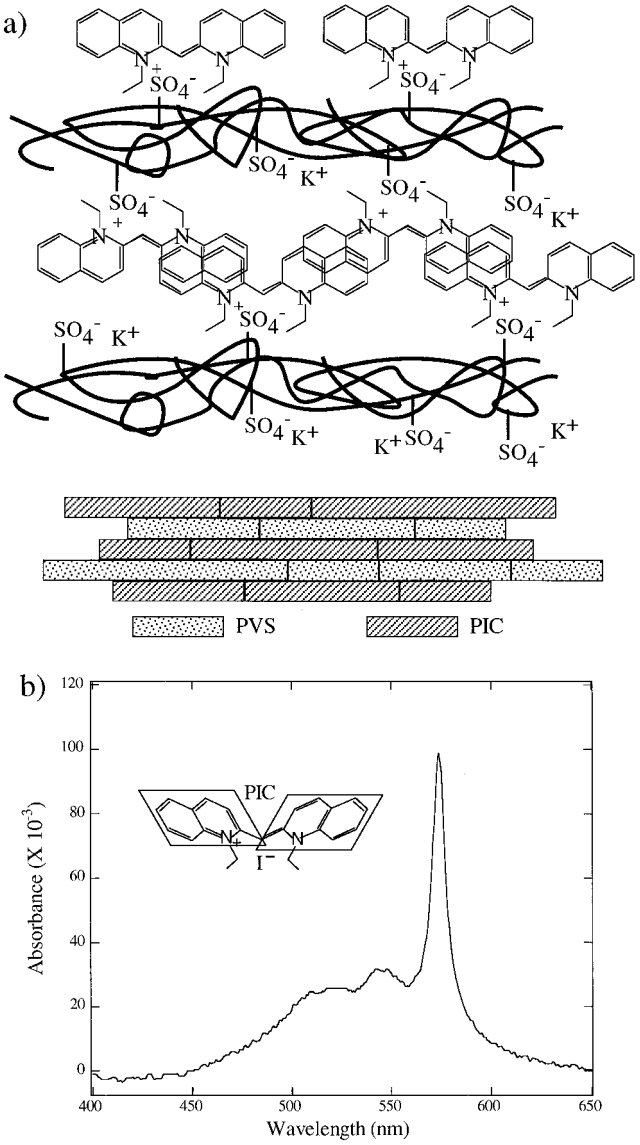


**FIGURE 3. (a) Schematic of a dye/polymer (PIC/PVS) self-assembly structure. (b) Absorption spectra of a thin film like the one shown in Figure 2d−i, and the molecular structure of the PIC dye.**

This circular aggregate nicely demonstrates that the fluorescence is strongly polarized along the long direction of the fibers. Excitation polarization experiments show the absorption is polarized in the same direction at long excitation wavelengths, but that it is polarized in the perpendicular direction at shorter excitation wavelengths. These and related measurements demonstrate that the dye molecules are organized in the usual distorted brickstone arrangement for PIC molecular aggregates with a herringbone-like arrangement of the molecular transition moments.[14]

The spatial variation of the fluorescence spectra of the aggregates shows the high degree of molecule order in the aggregates. The dispersed fluorescence as a function of tip position shows only slight variation (2 nm rms) along the aggregates.[13] This demonstrates that there is minimal inhomogeneous broadening of the spectra on the nanometer scale, leading to the conclusion (along with the polarization data) that there is a high degree of molecular order over many micrometers and on many distance scales! Thus, the molecular yarn is essentially bundles of

(12) Bohn, P. W. *Annu. Rev. Phys. Chem.* **1993**, *44*, 37.
(13) Higgins, D. A.; Barbara, P. F. *J. Phys. Chem.* **1995**, *99*, 3.
(14) Higgins, D. A.; Reid, P. J.; Barbara, P. F. *J. Phys. Chem.* **1996**, *100*, 1174.
(15) Higgins, D. A.; Kerimo, J.; Vanden Bout, D. A.; Barbara, P. F. *J. Am. Chem. Soc.* **1996**, *118*, 4049.
(16) Reid, P. J.; Higgins, D. A.; Barbara, P. F. *J. Phys. Chem.* **1996**, *100*, 3892.

one-dimensional liquid crystals that are frozen in a specific structure by the polymer matrix. We can find no closely related examples in the literature of this type of self-assembly. In some respects it represents wormlike micelles which also exhibit a one-dimensional order. The intermolecular interactions within an individual thread result in the uniform high degree of order that leads to the narrow-wavelength spectral characteristics of these aggregates. The interactions between the threads causes the apparent cross-linking of the fibers. This leads to the extensive yarn formation as well as the gel-forming ability of aqueous solutions of the aggregates.

For molecular aggregates, coupling of the tightly packed molecular transition moments leads to the formation of delocalized excited states (excitons) through the coherent excitation of a number of dye molecules.[12] For the PIC/PVS aggregates the spectroscopic data (Figure 3b) indicate an optical delocalization size of 25 monomers (a few nanometers). In addition to these coherent interactions, incoherent hopping of excitons through energy transfer during the excited state lifetime is an additional mechanism for energy migration along the aggregates. We have been able to show the high degree of fluorescence polarization of the aggregates in curved regions demonstrates that energy migration does not occur over more than 50 nm.[14]

Another means for estimating the distance scale for exciton migration is avilable in the spatial extent of tip-induced photochemistry (spatial hole-burning). This is shown in parts h and i of Figure 2, which are pairs of NSOM images recorded before and after photobleaching (induced photochemistry) in a localized stripe. Since the tip creates excitons locally that can migrate and decay by several mechanisms including photochemistry (e.g., photooxidation), the locally-photobleached image gives a direct image of the exciton migration distance if this distance is larger than the size of the tip. The dimensions of the photobleached area are approximately that of the irradiated area, yielding an estimate of ~50 nm as an upper limit for exciton migration in these aggregates.[13] Additionally, time-resolved NSOM experiments show the exciton lifetime to be shorter than 10 ps, severely limiting the extent of possible exciton migration.[16]

The PIC/PVS experiments also lead to some general conclusions for the application of NSOM to organic materials research. A combination of spectroscopic, polarization, photobleaching, and time-resolved NSOM experiments is required to obtain an accurate picture of the structure and properties under investigation. The correlation of optical properties and topography is a powerful means of determining mesostructure. Even though NSOM is limited to tens of nanometers near the surface of a sample, it is not strictly a surface technique in the molecular sense. This is an advantage in many cases, such as LEDs, where the bulk optical properties are of greater interest than those specifically limited to molecules at the surface.

**Spatially Resolved Spectral Inhomogeneities in Microcrystals.** One of the real powers of NSOM is the correlation of spectral bandshape with spatial position. This is not a factor in the PIC/PVS aggregates since their spectra do not vary with position along the aggregate. The opposite is true of single crystals of PIC, which exhibit tremendous variations in their fluorescence spectra with position.[17] The results are summarized in Figure 4a−e. PIC crystals have already been studied by far-field spectroscopic means and are a benchmark for understanding the optical properties of ordered dye arrays.[18] Our studies were the first to report spectra of nanocrystals grown under conditions that led to a very different morphology than the large crystals previously studied. The crystals are approximately 10−20 $\mu$m long, 5 $\mu$m wide, and 400 nm thick. The surface of the crystal is characterized by terraces of thin plates. The topography (Figure 4a) and polarized NSOM images (not shown) indicate that the crystals are composed of platelike single crystalline domains (~20 nm thick) separated by defect planes that extend throughout the crystal. Despite the uniformity of the polarization throughout the crystals, the fluorescence spectra (Figure 4e) depend dramatically on the location of the NSOM tip over the sample (Figure 4b). The spectra show two distinct emission bands that have been assigned to the expected bulk PIC crystal emission (620 nm) and emission from lower energy emissive (700 nm) traps caused by local structural dislocations. Parts c and d of Figure 4 are excitation images of the bulk crystals (620 nm) and the detects (700 nm), respectively. The images dramatically demonstrate that the latter species are observed to form in distinct regions. The correlation of the NSOM and topography demonstrates the 700 nm emitting defects are located at the interface of the crystal plates; e.g., the 700 nm emission is stronger when the tip goes down in holes in the upper layer. The NSOM fluorescence images correlate with the surface topography but not the total crystal thickness. This is because these crystals are strongly absorbing at the excitation wavelength and they absorb most of the light in the first 100 nm. Additional variations are observed as a function of tip position in the band maxima of the ~600 nm emission as a result of environmental inhomogeneities. Approximately 100 $cm^{-1}$ of broadening in the far-field, bulk spectrum (Figure 4f) is due to spectral inhomogeneities that occur on the >100 nm distance scale.

The PIC crystal studies clearly demonstrate the ability of NSOM to isolate spatial regions with unique spectral properties both within and perpendicular to the plane of the sample. With its high resolution and single-molecule sensitivity, NSOM can spatially probe extremely small spectral regions. All of these abilities make NSOM invaluable in studying how the electronic and optical properties of materials vary over small distance scales.

A different application of NSOM, in progress in our laboratory, is the study of energy migration and electron transfer across nanostructured interfaces. The work is focused on an absorbing layer of PPEI nanocrystals lying on an underlayer of titanyloxyphthalocyanine (TiOPc). Parts g and h of Figure 4 show topographic and fluorescence NSOM images of just the PPEI crystals on glass. The corresponding data for PPEI on a continuous polycrys-

(17) Vanden Bout, D. A.; Kerimo, J.; Higgins, D. A.; Barbara, P. F. *J. Phys. Chem.* **1996**, *100*, 11843.
(18) Marchetti, A. P.; Salzberg, C. D.; Walker, I. P. *J. Chem. Phys.* **1976**, *64*, 4693.

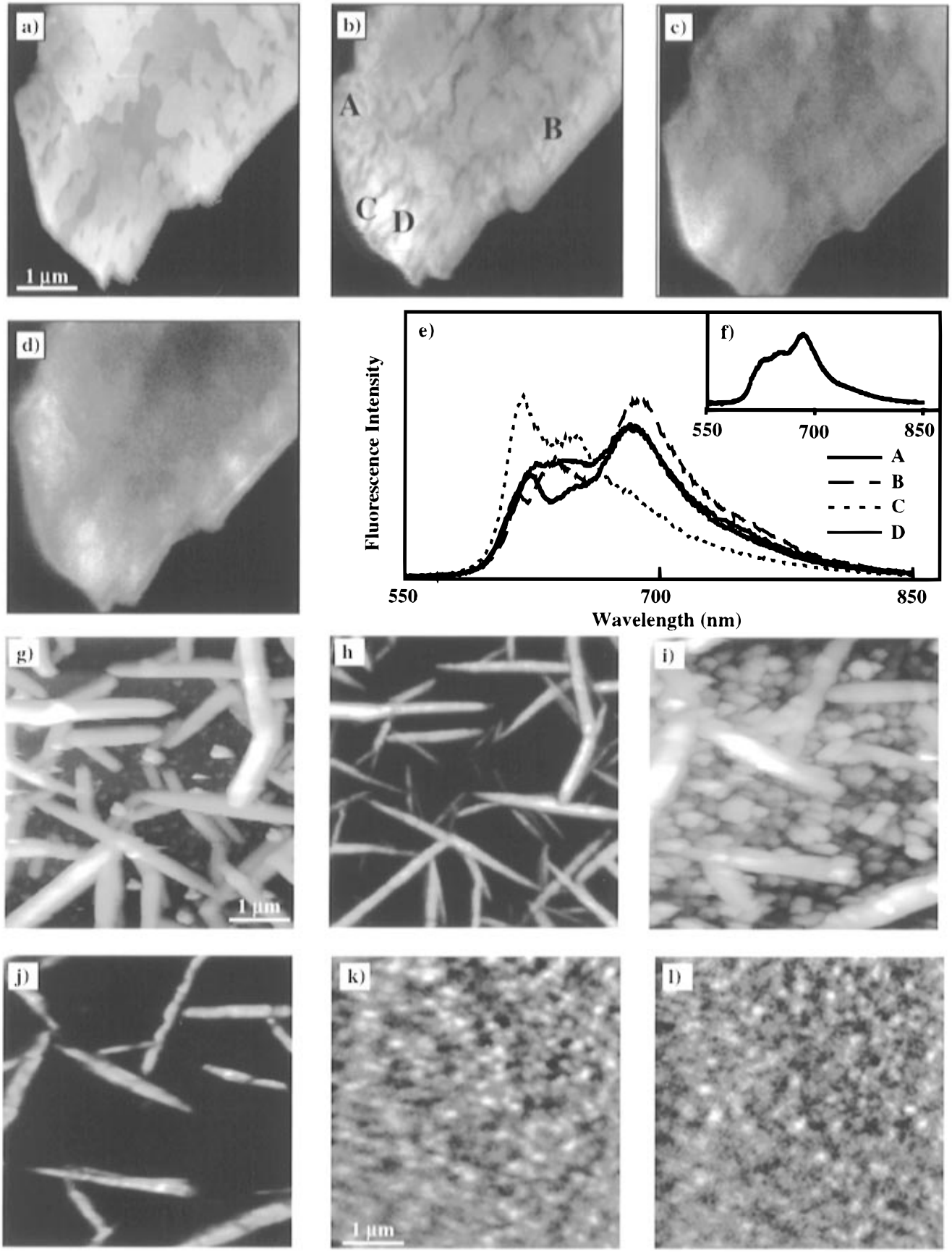


**FIGURE 4. (a–d) NSOM images of small PIC dye crystals: (a) topography, (b) total emission, (c) 620 nm emission, (d) 700 nm emission. (e) Fluorescence spectra recorded in the near field for the PIC crystal. Letters denote spatial locations identified in Figure 4b. (f) Far-field spectrum. (g–j) NSOM images of PPEI crystals: (g) topography and (h) fluorescence NSOM of PPEI crystals on glass, (i) topography and (j) fluorescence NSOM of PPEI crystals on a TiOPc layer. (k,l) NSOM images of a thin film of PPyV: (k) horizontal fluorescence, (l) vertical fluorescence.**

talline layer of TiOPc (quencher) are shown in Figure 4i,j. The "chemical contrast" in the fluorescence NSOM image allows for the assignment of the topographic features to different chemical species. The fluorescence NSOM

images of PPEI on glass show uniform fluorescence along the crystals. In contrast, the images of the PPEI/quencher system exhibit larger variations in intensity. These dark spots are due to both efficient quenching of the PPEI fluorescence by the TiOPc underlayer and local variations in the concentrations of the PPEI and TiOPc.[19]

**Emitting Conjugated Polymers.** Conjugated polymer based light-emitting diodes are of intense commercial and fundamental interest. Typical devices are composed of a layered arrangement of electrode/electroluminescent polymer layer/electrode/support. A detailed understanding of the underlying structure, photophysics, and even photochemistry is required to make improvements in the polymer LEDs. Toward these goals we have been investigating individual polymer thin films supported on glass substrates with transmission and fluorescence NSOM.[20] In particular we have been investigating polymers related to poly(*p*-pyridylvinylene) (PPyV). A common approach to the construction of polymer LEDs is to simply spin coat thin amorphous layers of the polymer on top of an electrode and evaporate the other electrode on top of the polymer layer. Generally, this has been viewed as being desirable since such films are optically clear, flat, and less subject to cracking than more molecularly ordered arrangements. In addition, it has been proposed that molecular aggregation in the films can be detrimental to the electro- and photoluminescence efficiency of the these films.

Parts k and l of Figure 4 show fluorescence NSOM images of a spin-coated film of PPyV. Topographic images of the film indicate that the film is approximately 50 nm thick, relatively flat (2 nm rms), and free of any long-range order or obvious crystalline domains. In contrast, the polarized fluorescence NSOM images (Figure 4k,l) show clear features that have a characteristic size of approximately 200 nm. Importantly, the NSOM images differ strongly from the topographic images, indicating that the variations in emission intensity are not due to a difference in sample thickness. The images for the perpendicular polarizations are clearly different, suggesting that the fluorescence results from locally oriented regions of the sample with a "locally" preferred direction of absorption/emission. While a few of the images show evidence of weak bulk alignment of the locally oriented domains, the films are usually isotropic on a >200 nm distance scale. A related report of 100−300 nm domains in the transmission NSOM of conjugated polymer films has recently been published.[21]

## NSOM/Topographic Effects

Image contrast in NSOM occurs by a variety of mechanisms and is complicated by several factors.[22−25] One particularly difficult to interpret NSOM contrast effect is the so-called topographic artifact. This artifact results because the near-field intensity is a strong function of the tip/sample separation and it cannot be held fixed during a scan over sharply varying topographic features. An interesting example of this effect is the dark lines that exactly correspond to the edges of the PIC crystal plates in Figure 4b. As the tip scans off the edge of a 20 nm plate, the aperture moves off the crystal before the entire tip is clear of the edge. Because the electric field strength drops dramatically as a function of distance from the near-field aperture, when the tip is held at a higher distance, the fluorescence signal from the crystal is significantly lower. Interestingly, NSOM/topographic coupling can actually add a richness to the data that can aid in interpreting the results. For example the 700 nm NSOM fluorescence images do not exhibit the dark lines at the crystal edges, indicating that the defects are not in the near field of the tip but rather in the far field. This is consistent with the interpretation that the defects are located at the interfaces of the plates.

## Polarization-Modulation NSOM (PM-NSOM)

Polarization-dependent NSOM imaging provides a valuable tool for characterizing the local structure of thin films.[14,23,26] The magnitude of a polarization anisotropy (absorbance and/or fluorescence) in the sample and the direction of this anisotropy can lead to information on the local molecular orientation, photophysical structure, and dynamics. Polarization-dependent NSOM images recorded with linearly polarized light of a fixed polarization direction (e.g., Figure 2f,g) can provide useful information. However, polarization-modulation NSOM (PM-NSOM) which rotates the polarization of light from the tip at high frequency provides far more information in considerably less time.[26,27] Parts a−e of Figure 5 show PM-NSOM data for nanocrystals of rhodamine 110 using a new technique we recently reported in which the linearly polarized light that is coupled into the NSOM probe is rotated through an angle of 180° at a frequency of 2 kHz.[27] The anisotropic optical properties of the sample (due to dichroism, birefringence, and spatial anisotropic variations in the refractive index) produce a polarization-dependent modulation in the intensity of the near-field light coupled by the sample to the detector. Lock-in detection yields images of the amplitude and phase of the polarization-dependent response of the sample.

For PM-NSOM of strongly absorbing samples, such as rhodamine 110 imaged at 514 nm, the primary contrast mechanism is absorption of the near-field light. The amplitude (Figure 5b) is an approximate measure of the magnitude of the anisotropic absorbance while the phase (Figure 5d) yields an image of the local direction of the absorbance anisotropy. The phase image gives a local measure of $2\phi$ where $\phi$ is the orientation of the transition moment relative to the vertical direction of the image. Arrows that indicate the transition dipole direction can

(19) Adams, D. M.; Kerimo, J.; Zaban, A.; Gregg, B. A.; Barbara, P. F. *Abstr. Pap.—Am. Chem. Soc.* **1997**, *213*, 268-PHYS.
(20) Blatchford, J. W.; Gustafson, T. L.; Epstein, A. J.; Vanden Bout, D. A.; Kerimo, J.; Higgins, D. A.; Barbara, P. F.; Fu, D.-K.; Swager, T. M.; MacDiarmid, A. G. *Phys. Rev. B* **1996**, *54*, R3683.
(21) Nagahara, L. A.; Tokumoto, H. *J. Vac. Sci. Technol., B* **1996**, *14*, 800.
(22) Trautman, J. K.; Betzig, E.; Weiner, J. S.; DiGiovanni, D. J.; Harris, T. D.; Hellman, F.; Gyorgy, E. M. *J. Appl. Phys.* **1992**, *71*, 4659.
(23) Betzig, E.; Trautman, J. K.; Weiner, J. S.; Harris, T. D.; Wolfe, R. *Appl. Opt.* **1992**, *31*, 4563.
(24) Vaez-Iravani, M.; Toledo-Crow, R. *Appl. Phys. Lett.* **1993**, *62*, 1044.
(25) Valaskovic, G. A.; Holton, M.; Morrison, G. H. *J. Microsc.* **1995**, *179*, 29.
(26) Vaez-Iravani, M.; Toledo-Crow, R. *Appl. Phys. Lett.* **1993**, *63*, 138.
(27) Higgins, D. A.; Vanden Bout, D. A.; Kerimo, J.; Barbara, P. F. *J. Phys. Chem.* **1996**, *100*, 13794.

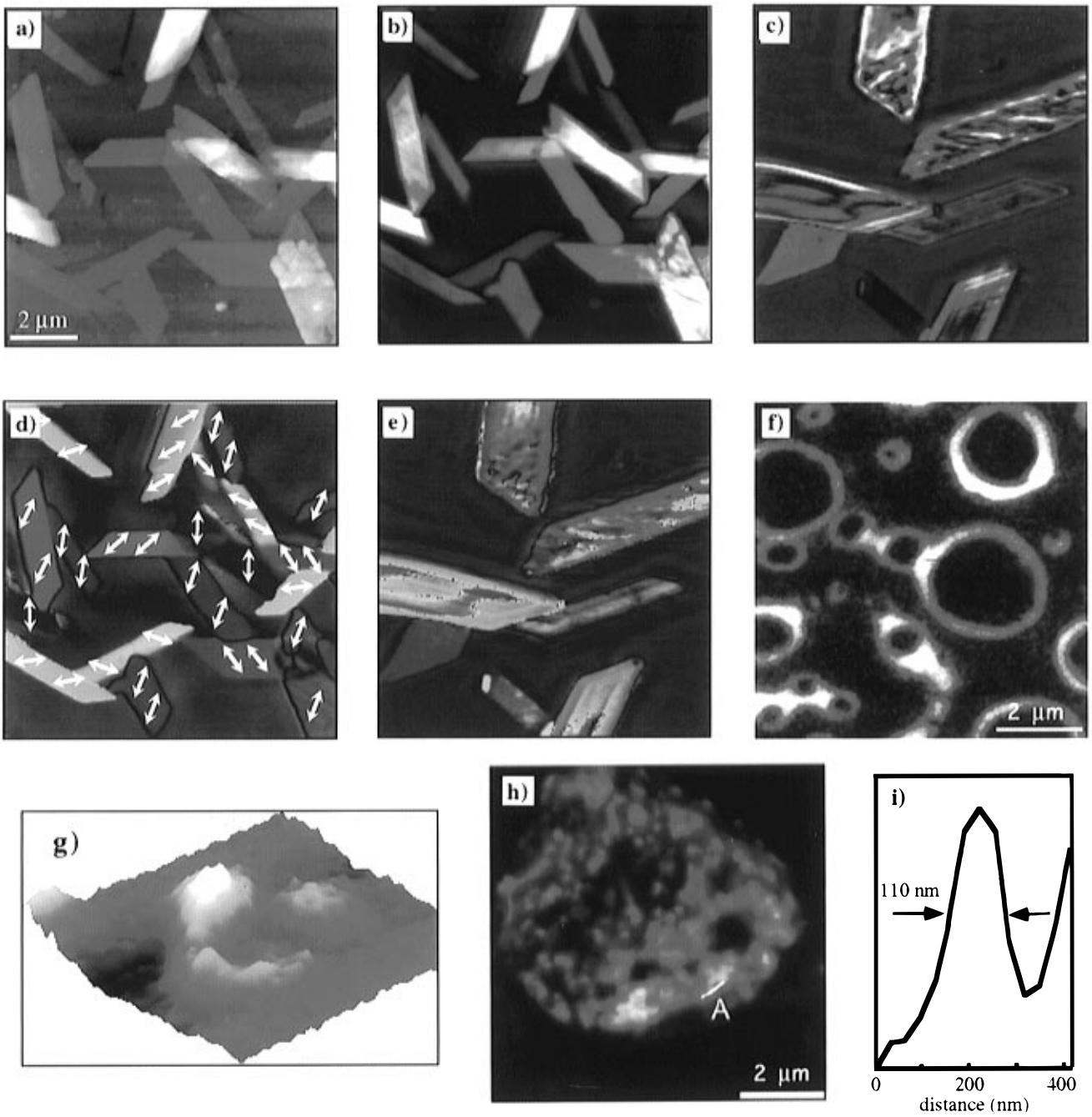


**FIGURE 5. PM-NSOM images of rhodamine 110 crystals: (a) topography, (b) amplitude, (c) off-resonant amplitude, (d) phase with dipoles, (e) off-resonant phase. (f) Fluorescence NSOM image of porphyrin rings (courtesy of F. DeSchryver). (g) Fluorescence NSOM image of an intact photosynthetic membrane (courtesy of X. Sunney Xie). Reprinted with permission from ref 46. Copyright 1994 American Chemical Society. (h) Fluorescence NSOM image of protein distribution in the membrane of an infected red blood cell (courtesy of S. Weiss). Reprinted with permission from ref 47. Copyright 1997 National Academy of Sciences. (i) Line scan of a small feature in image h.**

be superimposed on the phase image by using software to analyze the angle of orientation of strongly absorbing regions. Since the phase image of strongly absorbing samples yields the direction of the transition moment of the anisotropic absorbance, crystals of arbitrary orientation in the sample plane can be studied efficiently. It should be emphasized that the PM-NSOM yields a dramatic signal-to-noise-ratio improvement over nonmodulation measurements since the modulation of the signal moves it into a frequency range where the microscope has less noise associated with tip/sample distance and laser fluctuations.

As mentioned above, image contrast in NSOM is complicated by many factors. Nevertheless, for strongly absorbing samples the spatial variation in the NSOM transmission image empirically correlates with spatial variation in the absorbance of the sample over a limited range. For thick samples that extend beyond the near field, the NSOM absorbance can be due to absorption in both the near field and far field of the probe. Thus, transmission NSOM images of thick weakly absorbing samples must be interpreted with caution.

PM-NSOM imaging of samples at wavelengths for which there is no strong absorption offers a very different

set of advantages and disadvantages in characterizing mesostructured materials. Two major effects contribute to the contrast mechanism of this type of PM-NSOM. First, the local efficiency of coupling from the near field to the far field can depend on the local refractive index. Therefore, the anisotropy in the refractive index of birefringent samples ensures that the coupling will be polarization dependent. Second, even in a material with a locally isotropic refractive index, an anisotropic spatial variation in the refractive index (for example, small cracks) will cause the NSOM near-field/far-field coupling efficiency to be polarization dependent. Consider the PM-NSOM images of the rhodamine 110 recorded with 633 nm light (Figure 5c,e) which is only weakly absorbed by these crystals. The crystals appear bright relative to the glass background due to their birefringence, and edges and cracks show sharp NSOM features. A unique characteristic of PM-NSOM of nonabsorbing samples is that it only monitors the sample in the near field. Thus, it can be used for samples of arbitrary thickness. In this regard it is reminiscent of total internal reflection far-field methods, but for PM-NSOM the near-field aperture determines the penetration depth.

## Other NSOM Research

Extensive research on NSOM and its applications is taking place in many laboratories worldwide. Due to the short format of *Accounts* articles, it is not possible to exhaustively review all of the applications of NSOM to date. In particular, the very successful applications of NSOM to inorganic materials is beyond the scope of this paper.[5,28−30] Monolayer organic thin films have been studied by fluorescence NSOM including dye-doped phospholipid Langmuir−Blodgett films[31] and fluorescing polydiacetylene films,[32] leading to data on the morphology of these films. NSOM has recently been used to study "porphyrin wheel" aggregates. In contrast to the PIC aggregate rings (Figure 2f,g), the porphyrin wheels are assembled by a mechanism that produces a randomly oriented polycomposite of nanocrystals and the fluorescence from the rings is unpolarized (Figure 5f).[33] Another interesting direction is to use NSOM to control photochemistry on the submicrometer or smaller scale,[34,35] including the spatial-hole-burning studies (see above). Due to space limitations we have also not been able to deal with many other exciting areas of NSOM research, including NSOM methods that use non-optical-fiber tips,[36] NSOM approaches that employ bent fiber tips,[37,38] reflection mode NSOM,[39] NSOM Raman spectroscopy and imaging,[40−44] and NSOM methods with unique contrast mechanisms such as forbidden light microscopy.[45]

## Biological NSOM

NSOM of biological systems is beginning to make real progress. Figure 5g shows a fluorescence NSOM image of intact photosynthetic membranes.[46] Along with the spatial resolution of the NSOM-induced emission, the lifetime of the fluorescence has also been recorded, opening the door to a detailed spatial understanding of the photophysics of the entire photosynthetic apparatus. These measurements were performed under water with no obvious decrease in image quality, which is encouraging from the standpoint of applying NSOM to many biological and material science problems. NSOM is also improving the limits of resolution in cellular visualization. Figure 5h shows a fluorescence NSOM image of a an infected red blood cell. The image shows the distribution of a malaria protein within the erythrocyte membrane with a resolution of approximately 100 nm (Figure 5i).[47] Fluorescence NSOM has also been applied to in situ hybridization of human chromosomes, as a higher spatial resolution alternative to confocal methods.[48]

## NSOM Single-Molecule Spectroscopy

One of the most active and exciting areas of NSOM work has been fluorescence NSOM studies of single molecules. This work has been concerned with the spectroscopy, imaging, and dynamics of single dye molecules.[6−11] From the NSOM perspective, single-molecule studies have been critical in characterizing the near-field intensity distributions, demonstrating state-of-the-art fluorescence sensitivity, exploring tip/sample radiative and nonradiative interactions, and establishing good NSOM benchmarks. Recent NSOM work has led to the conclusion that, for single-molecule spectroscopy, confocal microscopy is better due to the confocal's higher signal-to-noise ratio.[49,50] However, for imaging applications, NSOM offers better


(28) Rogers, J. K.; Seiferth, F.; Vaez-Iravani, M. *Appl. Phys. Lett.* **1995**, *66*, 3260.
(29) Grober, R. D.; Harris, T. D.; Trautman, J. K.; Betzig, E.; Wegscheider, W.; Pfeiffer, L.; West, K. *Appl. Phys. Lett.* **1994**, *64*, 1421.
(30) Hess, H. F.; Betzig, E.; Harris, T. D.; Pfeiffer, L. N.; West, K. W. *Science* **1994**, *264*, 1740.
(31) Hwang, J.; Tamm, L. K.; Bohm, C.; Ramalingam, T. S.; Betzig, E.; Edidin, M. *Science* **1995**, *270*, 610.
(32) Moers, M. H. P.; Gaub, H. E.; van Hulst, N. F. *Langmuir* **1994**, *10*, 2774.
(33) De Schryver, F. C.; De Feyter, S.; Grim, K.; Faes, H.; Hofkens, J.; Jeuris, K.; Latterini, L.; Nolte, R. J.; Rowan, A.; Ruiter, M.; Schenning, A.; Vanoppen, P. *Abstr. Pap.—Am. Chem. Soc.* **1997**, *213*, 356-PHYS.
(34) Rucker, M.; Vanoppen, P.; De Schryver, F. C.; Horst, J. J.; Hotta, J.; Mashurhara, H. *Macromolecules* **1995**, *28*, 7530.
(35) Wei, P. K.; Hsu, J. H.; Hsieh, B. R.; Fann, W. S. *Adv. Mater.* **1996**, *8*, 573.
(36) Zenhausern, F.; Martin, Y.; Wickramasinghe, H. K. *Science* **1995**, *269*, 1083.
(37) Ben-Ami, U.; Tessler, N.; Ben-Ami, N.; Nagar, R.; Fish, G.; Lieberman, K.; Eisenstein, G.; Lewis, A.; Nielsen, J. M.; Moeller-Larsen, A. *Appl. Phys. Lett.* **1996**, *68*, 2337.
(38) Talley, C. E.; Cooksey, G. A.; Dunn, R. C. *Appl. Phys. Lett.* **1996**, *69*, 3809.
(39) Weston, K. D.; DeAro, J. A.; Buratto, S. K. *Rev. Sci. Instrum.* **1996**, *67*, 2924.
(40) Tsai, D. P.; Othonos, A.; Moskovits, M.; Uttamchandani, D. *Appl. Phys. Lett.* **1994**, *64*, 1768.
(41) Webster, S.; Smith, D. A. M.; Ayad, M. W.; Kershaw, K.; Batchelder, D. N. In *Proceedings of the International Conference on Raman Spectroscopy*; Asher, S. A., Stein, P. B., Eds. Wiley: New York, 1996; p 1146.
(42) Jahncke, C. L.; Paesler, M. A.; Hallen, H. D. *Appl. Phys. Lett.* **1995**, *67*, 2483.
(43) Jahncke, C. L.; Hallen, H. D.; Paesler, M. A. *J. Raman Spectrosc.* **1996**, *27*, 579.
(44) Emory, S. R.; Nie, S. *Anal. Chem.*, submitted for publication.
(45) Heinzelmann, H.; Hecht, B.; Novotny, L.; Pohl, D. W. *J. Microsc.* **1995**, *177*, 115.
(46) Dunn, R. C.; Holtom, G. R.; Mets, L.; Xie, X. S. *J. Phys. Chem.* **1994**, *98*, 3094.
(47) Enderle, T.; Ha, T.; Ogletree, D. F.; Chemla, D. S.; Magowan, C.; Weiss, S. *Proc. Natl. Acad. Sci. U.S.A.* **1997**, *94*, 520.
(48) Moers, M. H. P.; Ruiter, A. G. T.; van Hulst, N. F. *Zool. Stud.* **1995**, *34*, 21.
(49) Trautman, J. K.; Macklin, J. J. *Chem. Phys.* **1996**, *205*, 221.
(50) Macklin, J. J.; Trautman, J. K.; Harris, T. D.; Brus, L. E. *Science* **1996**, *272*, 255.

spatial resolution and straightforward coupling of topographic and optical images.

## Conclusion and Summary

NSOM combines the richness of optical spectroscopy with scanning probe microscopy. This has allowed NSOM to reveal unexpected mesostructures for a variety of types of materials, ranging from molecular aggregates, to single nanocrystals, to polymer thin films. The versatility of NSOM is increased by new tools such as PM-NSOM[27] and spatial hole-burning.[13] Despite the complexity of the contrast mechanisms, NSOM images can be assigned by careful study with several NSOM techniques and by correlation to simultaneous topographic measurements. This makes NSOM a unique and effective tool for the investigation of the mesostructure and localized photophysics of organic thin films.

*This research has been supported by the Office of Naval Research and the 3M Corp. D.A.V.B. and D.A.H. acknowledge NSF postdoctoral fellowships in chemistry. We thank our collaborators and co-workers including Phil Reid, David Adams, Art Epstein, Tim Swager, and Brian Gregg. We also thank Sunney Xie, Jay Trautman, Shimon Weiss, and Frans DeSchryver for helpful discussions. Numerous individuals at Topometrix are gratefully acknowledged for their advice on NSOM.*

AR960274K